EFDA–JET–PR(13)54

A.J. Webster, S.J. Webster
and JET EFDA contributors

ELM Processes and Properties in 2T 2MA JET Plasmas

ELM Processes and Properties in 2T 2MA JET Plasmas

A.J. Webster[1], S.J. Webster[1]
and JET EFDA contributors*

JET-EFDA, Culham Science Centre, OX14 3DB, Abingdon, UK

[1]*EURATOM-CCFE Fusion Association, Culham Science Centre, OX14 3DB, Abingdon, OXON, UK*
** See annex of F. Romanelli et al, "Overview of JET Results", (24th IAEA Fusion Energy Conference, San Diego, USA (2012)).*

Preprint of Paper to be submitted for publication in
Nuclear Fusion

ABSTRACT

During July 2012, 150 almost identical H-mode plasmas were consecutively created in the Joint European Torus (JET), providing a combined total of approximately 8 minutes of steady-state plasma with 15,000 Edge Localised Modes (ELMs). In principle, each of those 15,000 ELMs are statistically equivalent. Here the changes in edge density and plasma energy associated with those ELMs are explored, using the spikes in Beryllium II (527 nm) radiation as an indicator for the onset of an ELM. Two timescales are found during the ELM process. The first timescale is associated with the density drop, and the second (longer) timescale is associated with a reduction in MHD energy that is consistent with a resistive relaxation of the plasma's edge. The statistical properties of the energy and density losses due to the ELMs are explored. Surprisingly the commonly reported link between ELM energy (E) and ELM frequency (f), of $E \propto 1/f$, is not found. Instead beyond the first 0.02 seconds of waiting time between ELMs, the energy losses due to the ELMs are found to be statistically the same. Surprisingly no correlation is found between the energies of consecutive ELMs either. A weak link is found between the density drop and the ELM waiting time. Consequences of these results for ELM control and modelling are discussed.

1. INTRODUCTION

Edge Localised Modes (ELMs) are instabilities that occur at the edge of tokamak plasmas [1]. They are thought to be triggered by an ideal Magnetohydrodynamic (MHD) instability of the plasma's edge [2, 3], and are presently found in nearly all high confinement tokamak plasmas [4, 5, 6]. Large ELMs such as those that are predicted to occur in ITER [7, 8, 9], will need to be reduced in size or avoided entirely if plasma-facing components are to have a reasonable lifetime. One way to reduce ELM size is by "pacing" the ELMs at higher frequencies than their natural rate of occurrence [11, 10], because they are expected to occur with a lower energy due to the empirically observed relationship between ELM energy (E) and ELM frequency (f) of $E \propto 1/f$ [12]. The ELM frequency is usually reported as an average over all ELMs in a given pulse, and is identical to one divided by the average waiting time between the ELMs. In contrast to the relationships between the average ELM energy and average ELM frequency, the relationship between an individual ELM's energy and its individual "frequency" (often defined as one divided by its waiting time since the previous ELM), is rarely reported. It is this topic that is considered here.

Since 2011 the JET tokamak has been operating with its previously Carbon plasma-facing components replaced with the metal ITER-like wall [13]. This has led to differences in plasma confinement and ELM properties, as discussed for example in [13, 14] and references therein. This paper focuses its attention on a set of 150 JET plasmas produced over a two week period in July 2012, 120 of which were nearly identical, providing $\sim$10,000 statistically equivalent ELMs. Such high quality statistical information on ELM properties has never previously been available. The pulses are 2 Tesla 2 Mega Amp plasmas with approximately 12MW of NBI heating and roughly 6 seconds of steady H-mode, 2.3 seconds of which between 11.5 and 13.8 seconds is exceptionally steady and is what we consider here and in previous work [15, 16].

The outline of the paper is as follows. In Section 2 we describe how we determine and define the ELM sizes. In Section 3 we describe the statistical properties of the ELMs, and in Section 4 we discuss the results and propose our conclusions.

2. DEFINING THE ENERGY AND DENSITY DROP DUE TO AN ELM

The main purpose of this paper is to explore the relationship between the losses of plasma energy and density due to ELMs, and the waiting times between the ELMs. The signals that are used are the line averaged edge plasma density, which is a direct line-averaged measure of the density at the plasma's edge, and the plasma's ideal MHD energy as inferred from a collection of JET diagnostics. The Beryllium II (527nm) radiation that is measured at the inner divertor is used to determine when ELMs occur, using the method described in [17], that detects the statistically large spikes in the radiation that are associated with ELMs. For the type I ELMs in the H-mode plasmas considered here, the ELMs are easy to identify with this method. All the signals just described are

standard and widely used JET signals. Firstly we will discuss changes to the line averaged plasma density, similar remarks will apply to changes in the plasma's energy.

Following an ELM, the line averaged plasma density falls, then recovers again (see figure 1). The losses associated with the ELM have a duration of order 0.005 seconds, that combined with fluctuations in the signal can make it difficult to define the density loss due to the ELM. For example, figure 2 shows the fall in edge density with time since an ELM for ELMs in the typical pulse 83790. There is clearly a minimum at around 0.005 seconds, but the exact time and magnitude of the minimum is not always the same. Here we define the density drop due to an ELM (δn) as the maximum observed drop in the line-averaged density within a small time interval t_m after an ELM (see figure 4). Figure 4 shows that if δn is defined in this way then provided t_m is greater than about 0.005 seconds, which is much less than the 0.012 second waiting time to the most frequent ELMs [15, 16], then δn is independent of t_m. Consequently provided t_m is greater than 0.005 seconds, then δn is independent of t_m and is well defined. Unless specified otherwise, our plots use $t_m = 0.01$ seconds.

Similar remarks apply to the plasma's MHD energy, where the drop in energy (δE) is defined as the minimum energy in some time period t_m immediately following an ELM. A difference is that there are now two timescales that can clearly be observed (see figures 3 and 5). The first minimum in energy occurs between 0.002 and 0.005 seconds, which tends to be before the minima at 0.005s found in figure 4. However, unlike the density, there is a second minimum at around 0.01 seconds (see figure 3). The possible causes of the different timescales are discussed in greater detail later. Beyond 0.01 seconds the average of δE is approximately independent of t_m, allowing δE to be defined as the minimum energy in the time interval between an ELM and t_m=0.01 seconds (see figure 5). The choice of $t_m = 0.01$ seconds is less than the time of the first maxima in the ELM waiting time distribution [15, 16], that is at approximately 0.012 seconds. This definition defines the ELM energy as the total reduction in stored MHD energy due to the ELM, which is approximately three times larger than the energy lost during the initial 0.005 seconds, during which particle loss leads to a reduction in the edge density (see figures 4 and 5). Both minima can be observed in the time traces in figure 1, with a small minimum in δE prior to the minimum in the density, followed by a much larger minimum in δE on the larger timescale of ~ 0.01 seconds.

Two timescales have previously been reported in conjunction with the edge electron temperature during the post-ELM pedestal recovery [18, 19], an important difference is that here the two timescales are observed with every ELM. It is possible that the two timescales relate to a similar sequence of processes - rapid energy losses followed by slower transport processes. The timescale for the initial fall in edge temperature reported in Refs. [18, 19] is only about 0.002 seconds, whereas the drop in edge density (figures 2 and 4), is over a 0.005 second timescale. Two timescales have also been reported in conjunction with infra red (IR) images of JET's divertor [20]. In this latter work the two timescales arose from the shape of the ELM power deposition curve with respect to time, and are much shorter than those discussed so far. The timescales characterise the initial

rapid rise in ELM power deposition, over a timescale time $\tau_{rise} \sim 0.0002 - 0.0005$ seconds, and a slower $\tau_{decay} \sim 0.001 - 0.0025$ characterising the subsequent fall in the power deposition.

The work referred to above and the results here are consistent with, and possibly extend, the proposed sequence of steps by which energy is lost during an ELM [9]. Firstly there is a rapid rise in heat flux over a timescale of order 0.2-0.5 milliseconds [20], with heat being lost predominately by electrons until of order 1-2 milliseconds when the edge temperature reaches a minimum [18, 19]. This process of energy loss is referred to as "conduction" [9]. Next, for the plasmas described here at least, there is a loss of ions that is completed within a timescale of order 5 milliseconds (figure 4), in a process referred to as "convection" [9]. Finally we find an additional timescale of order 10 milliseconds after an ELM (figure 5), where the plasma continues to relax with a loss of stored energy, after which the stored energy starts to rise again. Appendix A explores the timescales associated with a resistive relaxation of the pedestal at the plasma's edge [21], and finds a timescale of 8 milliseconds, very similar to the 10 millisecond timescale within which the MHD energy relaxes to its minimum post-ELM value. Consequently it is possible that a resistive mechanism is allowing the plasma's MHD energy to relax to its minimum post-ELM value. It may also be significant that 8 milliseconds is the approximate time between the maxima and minima observed in the ELM waiting time pdf [15, 16], that will be observed later in the time periods between the clusters of ELMs in figures 6, 7 and 8.

3. STATISTICAL PROPERTIES OF ELMS

Next we look at how these measures of the density and energy losses associated with the ELMs are influenced by the waiting times between the ELMs (see figures 6 and 8). The most obvious characteristic of both figures is the vertical clustering of ELM times. This is due to the waiting-time probability density function (pdf), which is discussed in detail in Refs. [15, 16], and shows a series of maxima and zeros at approximately 0.08 second intervals starting from the first maxima at 0.012 seconds and continuing until 0.04 seconds when the distribution becomes comparatively smooth. The pdf was unexpected, and contrasts with large sets of ELM waiting time pdfs that have only a single maxima [17]. The cause of the unexpected form of pdf is unknown, and presently under investigation. The next striking characteristic of figures 6 and 8, that is particularly noticeable for the ELM energies, is that beyond a waiting time of about 0.02 seconds the ELM energies are similar and independent of the waiting time between the ELMs. In other words, the distribution of ELM energies that occur after a waiting time of 0.02 seconds is almost identical to those of ELMs with waiting times of 0.05 seconds or more. This is clearly different to the usual relationship of ELM energy being inversely proportional to ELM frequency [12], that would lead to the ELM energy being linearly proportional to the ELM waiting time. It is also despite a continual gradual increase in edge density that is suggested by figures 2 and 8. The first large group of ELMs are observed at 0.012 seconds, and these have an average energy that is roughly 60% of the ELMs in later groups. These results are similar to observations of pellet-triggered ELM energies in AUG

[22]. In the AUG pellet-triggering experiments, a minimum waiting time of 0.007-0.01 seconds was required before ELMs could successfully be triggered, and beyond roughly 0.01 seconds the triggered ELMs appear to have statistically similar energies [22]. It is unknown whether ELMs can be regularly triggered with waiting times less than the 0.012 second waiting time of ELMs in the group with the highest ELM frequency. Pellet pacing experiments in similar 2T 2MA JET plasmas [23], found a strong increase in triggering probability for pellets at least 0.01-0.02 seconds after an ELM. Due to technical limitations of the pellet launcher, it was not possible to test whether pellets could consistently pace ELMs with waiting times of order 0.012 seconds, but the possibility of triggering ELMs within those timescales was demonstrated. Therefore presuming ELMs can be paced at this 0.012 second waiting-time frequency, then an average reduction in ELM energy by about 40% seems a reasonable possibility. However there is a large scatter about the average ELM energy for all the ELMs, independent of their waiting time, with standard deviations that are about 1/4 of their average energy. Consequently some of the ELMs in the 0.012 seconds waiting-time group have ELM sizes comparable with the larger ELM sizes in the group with longer waiting times of 0.02 seconds or more.

Similar remarks apply to figure 7 where $t_m = 0.005$ seconds has been used. The time of $t_m = 0.005$ seconds corresponds to the first plateau of δE with t_m in figure 5, and is the timescale over which the edge density is lost (see figure 4). The group of ELMs at 0.012 seconds are about half the energy of later ones, which is comparatively less than for figure 6, and the overall ELM energies for waiting times greater than about 0.02 seconds are of order 40,000 Joules, which is about one third of the total energy lost from the plasma due to a typical ELM.

Figure 8 shows the drop in density (δn) due to the ELMs. Similar remarks apply as to those for the energy losses (figure 6), although in this case a weak dependence of δn on δt remains.

So why does the observed relation between ELM energy and ELM waiting times disagree with published studies [12] that find the ELM energy (E) to be inversely proportional to ELM frequency (f), with $E \propto 1/f$? The first and most important observations to make are that previous studies are usually plotting a pulse's average ELM energy against its average ELM frequency, and plotting these quantities for a variety of different pulse types. In contrast, here we are plotting the individual ELM energies against their waiting times (that can be regarded as defining 1/f for any given ELM), and doing this for these almost identical 2T, 2MA, pulses.

If we plot $\langle \delta E \rangle$ against $\langle \delta t \rangle$ for each of these pulses (see figure 9), we find a simple linear relationship that is consistent with $\langle \delta E \rangle \propto 1/f$, due to small differences in $\langle \delta E \rangle$ and $\langle \delta t \rangle$ in the different pulses. Figure 6 and the ELM waiting time pdf for these ELMs (as reported in [15, 16]), show that values of δE span an interval of about 10^5 Joules, and values of δt span an interval of about 0.1 seconds. The central limit theorem ensures that if all pulses are statistically equivalent, then the average of n ELMs should range over an interval that is proportional to $1/\sqrt{n}$ in width. For the roughly 50 ELMs in each pulse this would lead us to expect a range of values of $\langle \delta E \rangle$ within about $(0.14)10^5$ Joules, and values of $\langle \delta t \rangle$ to vary within a range of about 0.014

seconds. This is similar to what is observed in figure 9, but the spread of values is slightly greater, which indicates that the pulses are not quite statistically equivalent. In other words, the differences between the pulses are slightly greater than would be expected by chance alone, so the pulses are only approximately identical.

The observed linear relationship between $\langle \delta E \rangle$ and $\langle \delta t \rangle$ in figure 9 is not surprising. For the pulses here the spread of values of $\langle \delta t \rangle$ is small, with $\langle \delta t \rangle$ varying by no more than about $\pm$ 0.01 seconds. Consequently it would be unsurprising if a Taylor expansion of $\langle \delta E \rangle (\langle \delta t \rangle)$ were accurate with only the linear terms in $\langle \delta t \rangle$ being kept, consistent with the linear relationship observed in figure 9. In principle the observed linear relationship could reflect numerous possible different functions of $\langle \delta t \rangle$, not just a linear one. It is possible that if the pulses were of different types with very different values of $\langle \delta E \rangle$ and $\langle \delta t \rangle$, then plots of $\langle \delta E \rangle$ against $\langle \delta t \rangle$ would continue to show the linear relationship expected if $\langle E \rangle \propto 1/f$. However, what is clearly highlighted here is that even if the relationship of $\langle E \rangle \propto 1/f$ does hold between different types of plasma pulses, for the plasmas studied here at least, within a particular pulse the individual ELM energies can be independent of their waiting times (and the frequencies that they define).

A related question is whether the energies of subsequent ELMs are related to each other, or are independent. For example, we might expect a large ELM to be followed by a smaller ELM and vice versa. Figures 10 and 11 plot the energy of the nth ELM versus the energy of the (n+1)th ELM. If a large ELM is followed by a smaller ELM and vice versa, then we would expect the plotted values to cluster around a line that is perpendicular to the diagonal. The symmetric clustering about an average ELM energy suggests that the ELM energies (surprisingly) are independent. The same result was found for $t_m = 0.01$ seconds and $t_m = 0.005$ seconds, and when examining t_{n+m} versus t_n for $m = 1$ to $m = 5$.

4. DISCUSSION AND CONCLUSIONS

We have used the line averaged edge density and the MHD energy to study the properties of the $\sim$10,000 ELMs produced from 120 (of 150) almost identical JET pulses. It is found that: i) There are two clear timescales associated with the ELMs, the first involving a loss of density and energy, the second solely involving a loss of energy. Consequently the shorter timescale is likely to be important for the ELM energy flux onto material surfaces, whereas the longer timescale is likely to be important for the plasma's overall energy confinement. The longer 0.01 seconds timescale is a previously unreported timescale, after which the stored energy is found to start increasing again, and is similar to the 8 milliseconds resistive timescale of JET's plasma pedestal (see Appendix A). Consequently it is consistent with a resistive mechanism that allows the plasma's MHD energy to relax to a minimum value before recovering again. ii) Following an ELM, no ELMs are observed until approximately 0.012 seconds later, when they are statistically about 60% of the size of ELMs observed in the next cluster at approximately 0.02 seconds. Similar remarks apply regardless of whether the shorter or longer timescales of $t_m = 0.005$ seconds or $t_m = 0.01$ seconds are used. iii)

From 0.02 seconds onwards, the ELM energies are all statistically similar, with an approximately Gaussian distribution that is independent of the waiting times between the ELMs, and a standard deviation that is about 1/4 of the average ELM energy (see figures 12 and 13).

The first point (i), helps to clarify the processes taking place during an ELM that need to be better understood, and includes the observation of an extra relaxation time during the ELM process. Points (ii)-(iii) have clear consequences for ELM mitigation, at least for plasmas equivalent to those discussed here. The maximum (natural) ELM frequency that is observed has an ELM waiting time of approximately 0.012 seconds. ELMs with waiting times of $\simeq 0.012$ seconds have an average energy loss associated with the ELM that is roughly 60% that of the ELMs with waiting times of 0.02 seconds or longer. So presuming that ELM pacing techniques can consistently pace ELMs with waiting times of 0.012 seconds or less, then a reduction in average ELM energy by at least 40% seems likely to be possible, or 50% if the shorter timescale of $t_m = 0.005$ seconds is proportional to the peak heat fluxes onto surfaces. However, many of the ELMs are statistically expected to be much larger in size than average. In addition, the 83Hz frequency of these ELMs is faster than previous successful pacing experiments on JET, whereas for the ELMs observed here with frequencies of 50Hz or less, their expected energies are approximately the same.

The results summarised in figure 6 clearly fail to satisfy the often quoted relationship of $E \propto 1/f$. This may be partly because the relationship that is measured in such papers is actually $\langle E \rangle \propto 1/\langle f \rangle$, and consequently refers to average properties of possibly very different plasmas, and not to the properties of individual ELMs within similar plasmas. Unfortunately it is this latter quantity, the relationship between ELM size and ELM waiting time that is important for ELM mitigation by pacing techniques. Without a reduction in ELM energy, mitigation techniques will need to reduce either the peak heat flux or increase the wetted area onto which energy is deposited. The results presented here also only represent one particular type of pulse in one tokamak, JET. It is entirely possible that different pulse types or different machines might have very different ELM statistics. The purpose of the analysis here is to provide a robust analysis of these 2T 2MA pulses for which such large numbers of (almost) statistically equivalent ELMs are available, providing a clear indication of ELM behaviour for this particular pulse type at least. The hope was that the excellent statistics might indicate new or unexpected ELM physics. One of the unexpected results is the observed independence of ELM size and waiting time for waiting times greater than about 0.02 seconds. Similar observations were found in pellet-pacing experiments in AUG [22], where ELM sizes were similar for waiting times beyond roughly 0.01 seconds. The generality of these results remains to be determined, and may require dedicated new experiments to ensure a robust answer.

The results here have consequences for the correct construction of models for ELMs and ELM-ing behaviour. For the pulses discussed here, beyond the 0.012 seconds waiting time the ELM waiting times and energies are independent. Consequently for such ELMs, models to describe their waiting times and ELM-energy probability distributions can be treated independently. Even

more surprisingly perhaps, is that figures 10 and 11 suggest that the energies of subsequent ELMs are independent, so that a large ELM is as likely to be followed by another large ELM as by a small ELM. Surprising as this may be, it is likely to make the statistical modelling of ELM energies considerably easier. Clearly, the statistical relationships observed here need to be reproduceable by any simulation that is correctly modelling these plasmas. Similar remarks apply to the relaxation of the plasma's energy, and the sequence of processes and timescales by which the plasma loses energy due to an ELM.

To conclude, we have presented the analysis of an unprecedentedly large number of statistically equivalent 2T 2MA JET H-mode plasmas. This has led to the observation of an extra 0.01 second timescale associated with the ELM process, that is consistent with a resistive mechanism that allows the plasma to relax to its minimum post-ELM energy. For the plasmas discussed here, surprising results are reported about the independence of ELM energy and frequency, and the independence of energies of consecutive ELMs. Whether the results found here are more generally true is unknown, it may be some time before equivalently large datasets for different pulse types or from different machines become available.

Acknowledgments: Thanks to Martin Valovic for help with resistivity estimates, Ian Chapman for comments on the paper, and to Howard Wilson and Fernanda Rimini for raising the question of how the ELM energies are related to the waiting times for this set of pulses. The experiments were planned by S. Brezinsek, P. Coad, J. Likonen, and M. Rubel. This work, part-funded by the European Communities under the contract of Association between EURATOM/CCFE was carried out within the framework of the European Fusion Development Agreement. For further information on the contents of this paper please contact publications-officer@jet.efda.org. The views and opinions expressed herein do not necessarily reflect those of the European Commission. This work was also part-funded by the RCUK Energy Programme [grant number EP/I501045].

A. THE GLOBAL CURRENT RELAXATION TIMESCALE

As given in Ref. [24] for example, the plasma's resistivity is,

$$\eta = (6.5)10^{-8}\left(\frac{1}{T_k^{3/2}}\right)\ \Omega\ \mathrm{m} \tag{1}$$

where T_k is the plasma's temperature measured in electron Volts. A multiplicative constant modifies Eq. 1 when Neoclassical effects are included and if $Z_{eff} \neq 1$, but Eq. 1 is a reasonable order of magnitude estimate. The resistive MHD equations [24] give,

$$\frac{\partial \vec{B}}{\partial t} = \left(\frac{\eta}{\mu_0}\right)\nabla^2\vec{B} \tag{2}$$

from which a dimensional analysis gives the resistive timescale τ as,

$$\tau \sim \left(\frac{\mu_0}{\eta}\right)L^2 \tag{3}$$

where L is a typical length scale and $\mu_0 = (4\pi)10^{-7}$ Farad m^{-1}. Combining equations 1 and 3 gives,

$$\tau \sim (6.2)\pi T_k^{3/2} L^2 \tag{4}$$

Substituting the pedestal width [21] of $L \sim 0.03$m and temperature at the pedestal's top of $T_k \sim 0.6$keV, gives $\tau \sim 8$ milliseconds, very similar to the 10 millisecond timescale within which the MHD energy relaxes to its minimum post-ELM value.

REFERENCES

[1] J. Wesson $Tokamaks$ (Oxford University Press, Oxford, 1997).

[2] P.B. Snyder, R.J. Groebner, A.W. Leonard, T.H. Osbourne, H.R. Wilson, Phys. Plasmas **16**, 056118, (2009).

[3] A.J. Webster, Nuclear Fusion 52, 114023, (2012).

[4] M. Keilhacker, Plasma Phys. Control. Fusion, 26, 49 (1984)

[5] H. Zohm, Plasma Physics and Controlled Fusion 38, 105, (1996).

[6] Kamiya et al., Plasma Physics and Controlled Fusion 49, S43, (2007).

[7] R. Aymar et al. for THE ITER TEAM, Plasma Physics and Controlled Fusion 44, 519, (2002).

[8] B. Lipschultz, X. Bonnin, G. Counsell, et al. Nucl. Fusion **47**, 1189-1205, (2007).

[9] A. Loarte, B. Lipschultz, A.S. Kukushkin, et al. Nucl. Fusion **47**, S203-263, (2007).

[10] P.T. Lang, A. Loarte, G. Saibene, et al. Nucl. Fusion **53**, 043004, (2013).

[11] Y. Liang, Fusion Science and Technology 59, 586, (2011).

[12] A. Herrmann, Plasma Phys. Control. Fusion **40** (2002), 883-903.

[13] R. Neu, G. Arnoux, M. Beurskens, et al. Phys. Plasmas **20**, 056111, (2013)

[14] G.P. Maddison, C. Giroud, B. Alper, et al. submitted to Nucl. Fusion (2013).

[15] A.J. Webster, R.O. Dendy, F.A. Calderon, S.C. Chapman, E. Delabie, D. Dodt, R. Felton, T.N. Todd, V. Riccardo, B. Alper, S. Brezinsek, P. Coad, J. Likonen, M. Rubel, and JET EFDA Contributors "The Statistics of Edge Localised Modes", P4.112, 40th EPS Conference on Plasma Physics, Helsinki, Finland, 2013.

[16] A.J. Webster, R.O. Dendy, F.A. Calderon, S.C. Chapman, E. Delabie, D. Dodt, R. Felton, T.N. Todd, V. Riccardo, B. Alper, S. Brezinsek, P. Coad, J. Likonen, M. Rubel, and JET EFDA Contributors, submitted to Plasma Phys. Control. Fusion, (arXiv:1310.0287), 2013.

[17] A.J. Webster and R.O. Dendy, Phys. Rev. Lett. 110, 155004, (2013).

[18] M.N.A. Beurskens, L. Frassinetti, C. Maggi, et al. Submitted to Proceedings of 24th IAEA Fusion Energy Conference, San Diego, USA, 8th-13th October, (2012).

[19] L. Frassinetti, D. Dodt, M.N.A. Beurskens, et al. 40th EPS Conference on Plasma Physics, P5.183, (2013)

[20] H. Thomsen, T. Eich, S. Devaux, et al. Nucl. Fusion **51**, 123001, (2011).

[21] L. Frassinetti, M.N.A. Beurskens, R. Scannell et al. Rev. Sci. Instrum. 83, 013506, (2012).

[22] P.T. Lang, M. Bernert, A. Burckhart, et al. 40th EPS Conference on Plasma Physics, O2.102, (2013).

[23] P.T. Lang, D. Frigione, A. Geraud, et al. Nucl. Fusion **53**, 073010, (2013).

[24] J. Freidberg "Plasma Physics and Fusion Energy", Cambridge University Press, Cambridge, UK, (2007).

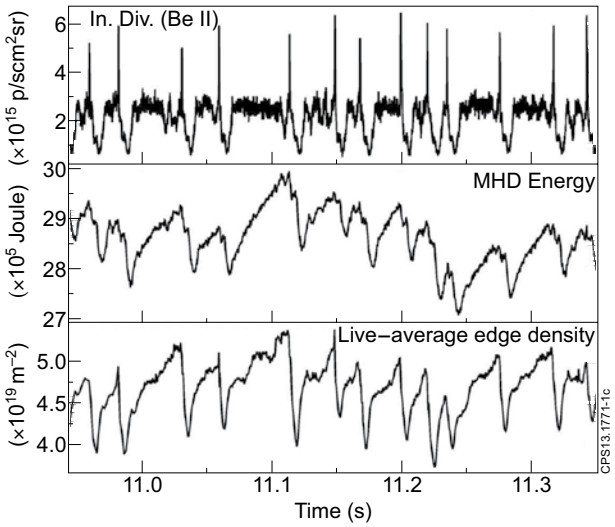

Figure 1: From top to bottom: i) The Be II (527nm) signal measured at the inner divertor, that is used to identify ELMs from the sharp spikes in radiation. ii) The Magnetohydrodynamic (MHD) energy stored in the plasma. iii) The line-averaged plasma number density at the plasma's edge. For each ELM there is a sharp spike in Be II emission, shortly followed by a drop in density to a minimum at around 0.005s after the ELM started, and a drop in MHD energy to a minimum some time around 0.01s after the ELM started.

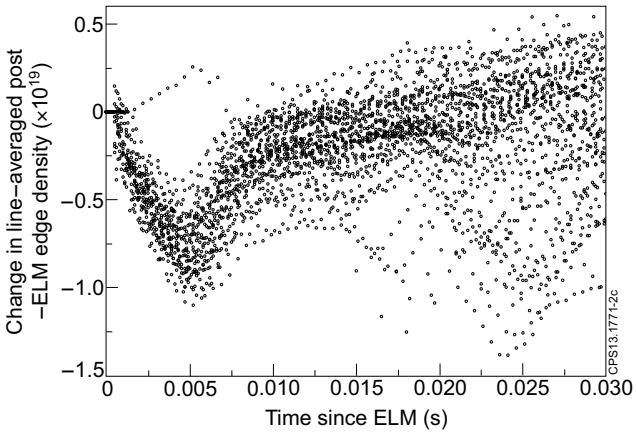

Figure 2: The fall in line-averaged edge density with time since each ELM is plotted for a typical pulse in the set (Pulse No: 83790). There is a clearly visible minima at around 0.005 seconds. Beyond about 0.012 seconds there are a small number of additional drops in density due to ELMs that occur within the 0.03 second time interval that is plotted.

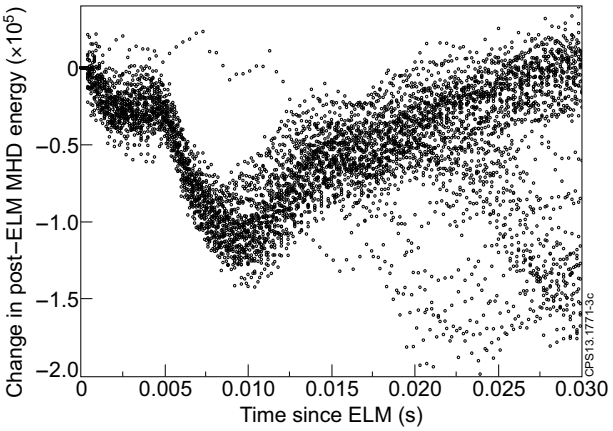

Figure 3: The fall in MHD energy with time since each ELM is plotted for a typical pulse in the set (Pulse No: 83790). There are two clearly visible minima, one between 0.002 and 0.005 seconds, and another at around 0.01 seconds. Beyond about 0.012 seconds there are a small number of additional drops in energy due to ELMs that occur within the 0.03 second time interval that is plotted.

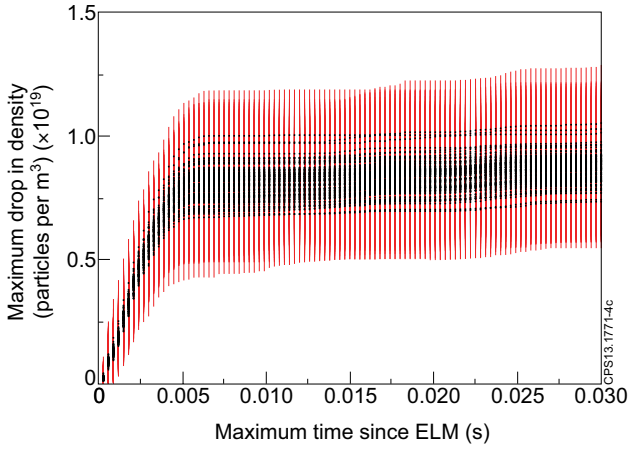

Figure 4: The maximum drop in line averaged plasma density (δn) following an ELM (vertical axis), is plotted against the (maximum) time tm since the ELM (horizontal axis), over which the maximum drop is calculated. For each plasma δn is averaged over all the ELMs in a given pulse (plotted points), and its standard deviation calculated (vertical lines). This is repeated for each maximum time t_m since the ELM, and for each plasma pulse. There is a comparatively small scatter of about 15-20% between the average value's of δn for the 120 different pulses, confirming that the pulses are quite similar. Consequently if tm is taken to be greater than about 0.005 seconds then there is a well defined δn that is independent of tm. The timescale of 0.005 seconds is much less than the time between ELMs.

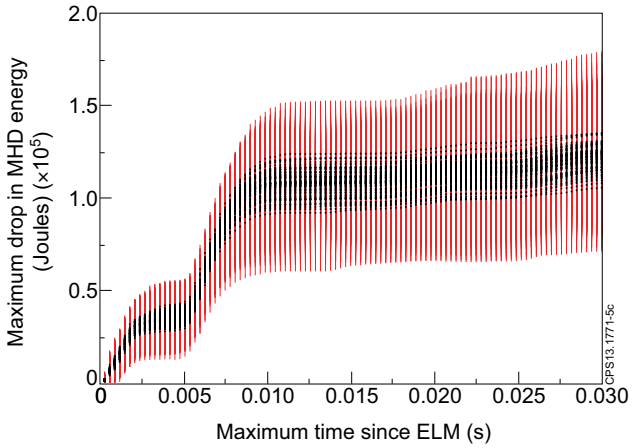

Figure 5: For tm from 0 to 0.03 seconds and for all 120 pulses, the minimum MHD energy within time tm after an ELM is averaged over all ELMs in a pulse (plotted points), and the standard deviation about this average is calculated also (vertical lines). The 120 sets of averages (plotted points) and standard deviations (red lines) have been plotted over one another so as to present them on a single graph. Two time scales are evident. The first at 0.005 seconds is the same as found in figure 4. The second timescale is at 0.01 seconds, beyond which the average value of δE is approximately constant, independent of t_m.

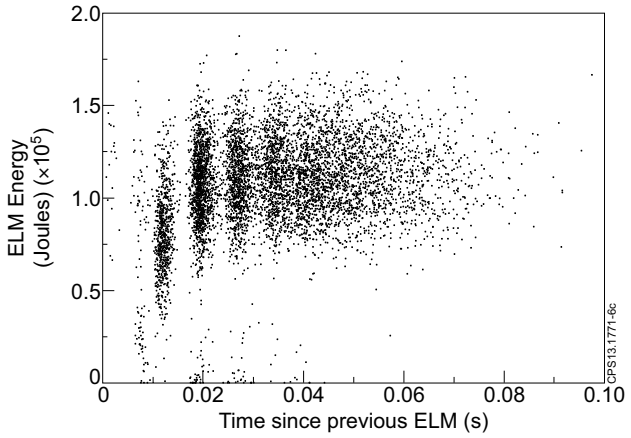

Figure 6: The drop in the plasma's ideal MHD energy is plotted against waiting time since the previous ELM. The vertical clustering is due to the unusual ELM waiting time pdf described in references [15, 16]. The stored MHD energy was of order $(2.8)\times10^6$ Joules, suggesting that of order 0.04% of the plasma's MHD energy is removed by each ELM. Beyond 0.02 seconds the ELM energies are approximately independent of the waiting time between the ELMs.

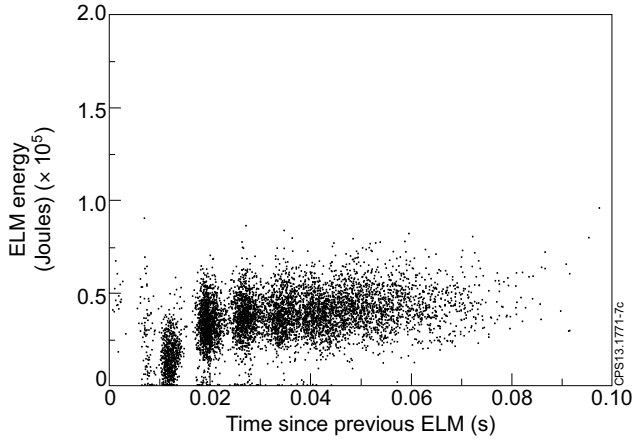

Figure 7: The drop in the plasma's ideal MHD energy is plotted against waiting time since the previous ELM, as in figure 6. Here however, δE has been calculated using $t_m = 0.005$ seconds, the time of the first plateau in δE versus t_m in figure 5, and the time beyond which the drop in edge density has ended.

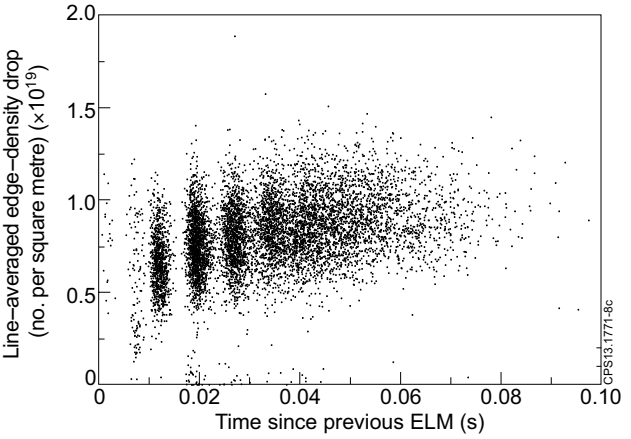

Figure 8: The drop in line averaged edge density is plotted against waiting time since previous ELM. Similarly to the plot of energy against waiting time, the vertical clustering is due to the unusual ELM waiting time pdf of the ELMs in these pulses, as described in references [15, 16]. The line-averaged edge density was of order $(4.5)10^{19}$, suggesting that roughly 20% of the edge density is lost per ELM. Beyond about 0.005 seconds the minimum observed drop in density is independent of tm. Beyond 0.02 seconds the drop in edge density due to an ELM is only very weakly dependent on the waiting time between ELMs.

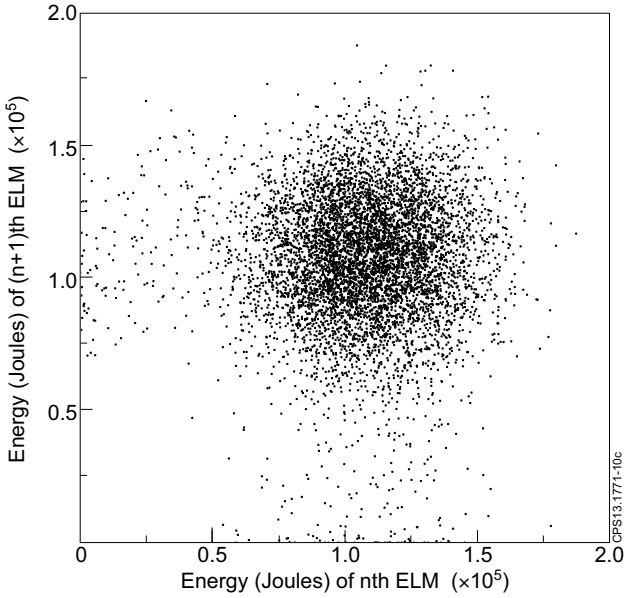

Figure 9: For each of the 120 pulses, the average ELM energy is calculated and plotted against the average ELM waiting time for that pulse. The scatter is slightly greater than would be expected from the central limit theorem and the roughly 50 ELMs per pulse, indicating that the pulses are only approximately statistically equivalent. The linear relationship observed between $\langle \delta E \rangle$ and $\langle \delta t \rangle$ is as expected if $\langle \delta E \rangle$ / 1/f, but for the small range of $\langle \delta t \rangle$ here it is also what would be expected from a simple Taylor expansion of $\langle \delta E \rangle(\delta t)$, and could in principle reflect numerous possible functions of δt.

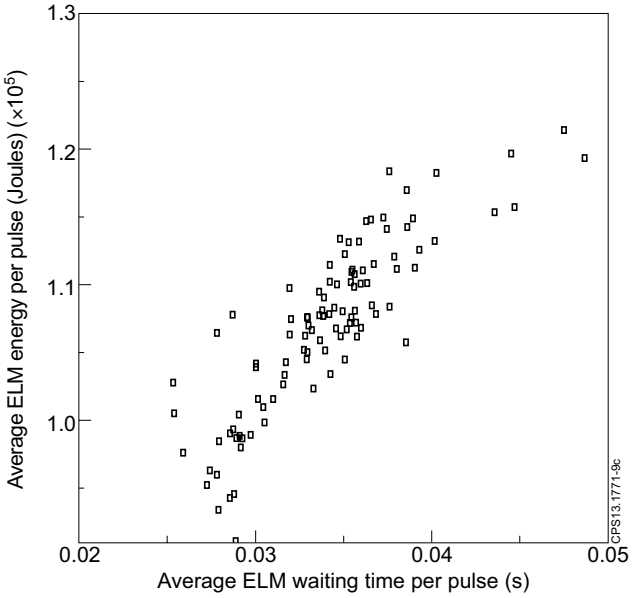

Figure 10: The energy of successive ELMs are plotted, with energies calculated using $t_m = 0.01$. Surprisingly, the clustering of subsequent ELM energies around a single point indicates that the energies of subsequent ELMs are independent. If a large ELM were followed by a small ELM and vice versa, then we would expect a spread of ELM energies in a perpendicular direction to the diagonal.

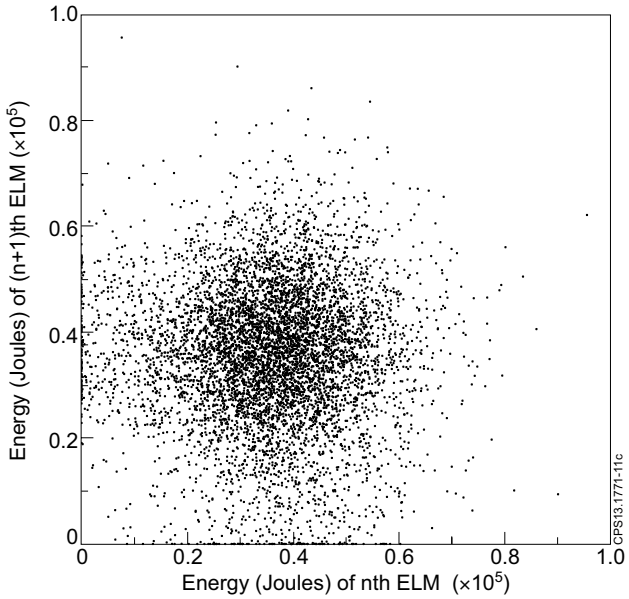

Figure 11: The energy of successive ELMs are plotted, with energies calculated using tm = 0.005. Surprisingly, the clustering of subsequent ELM energies around a single point indicates that the energies of subsequent ELMs are independent. If a large ELM were followed by a small ELM and vice versa, then we would expect a spread of ELM energies in a perpendicular direction to the diagonal.

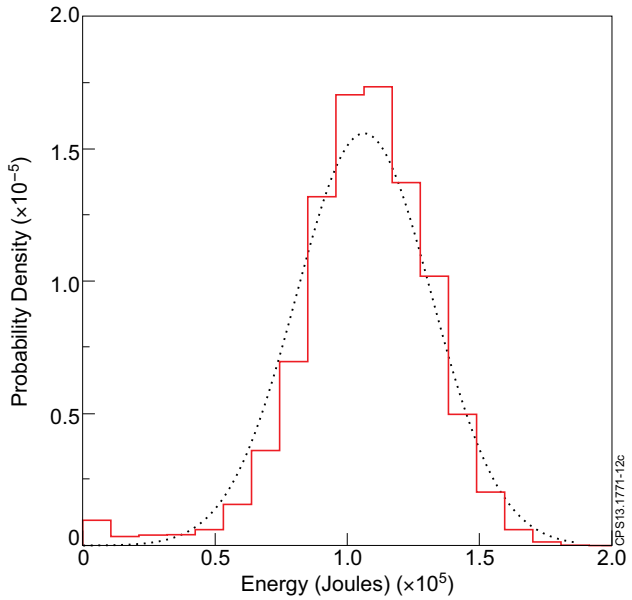

Figure 12: The probability density of ELM energies calculated with $t_m = 0.01$ is plotted, along with a simple Gaussian fit (dotted black curve). Even without excluding the ELMs that arise with waiting times less than roughly 0.02 seconds, the distribution of ELM energies is approximately Gaussian, with an average ELM energy of $(1.06)10^5$ Joules and a standard deviation of $(0.26)10^5$ Joules, giving a co-efficient of variation of 0.25 for the spread of ELM energies.

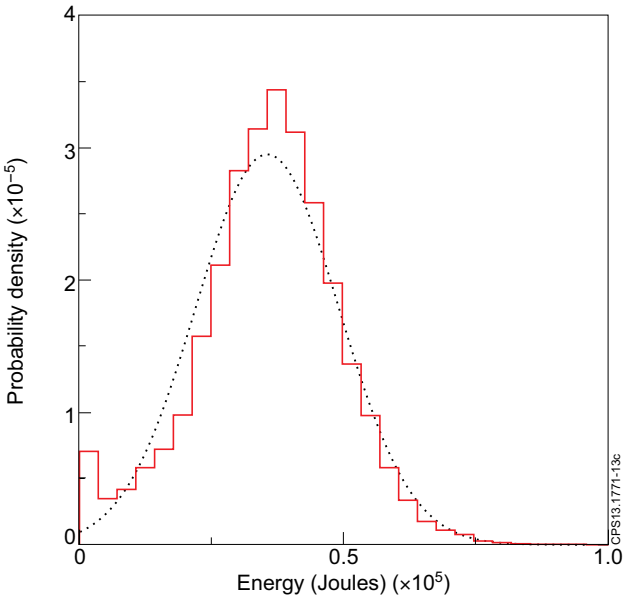

Figure 13: The probability density of ELM energies calculated with $t_m = 0.005$ is plotted, along with a simple Gaussian fit (dotted black curve). Even without excluding the ELMs that arise with waiting times less than roughly 0.02 seconds, the distribution of ELM energies is approximately Gaussian, with an average ELM energy of $(3.55)10^4$ Joules and a standard deviation of $(1.35)10^4$ Joules, giving a co-efficient of variation of 0.38 for the spread of ELM energies